

**REPUBLIC OF TURKEY
ISTANBUL GELISIM UNIVERSITY
INSTITUTE OF GRADUATE STUDIES**

Department of Electrical and Electronics Engineering

**PHOTOVOLTAIC CELL MODELING VIA
METAHEURISTIC ALGORITHMS**

Master Thesis

Ahmed Raed Azeez AZEEZ

Supervisor

Assoc.Prof.Dr. Indrit MYDERRIZI

Istanbul – 2022

THESIS INTRODUCTION FORM

Name and Surname : Ahmed AZEEZ

Language of the Thesis : English

Name of the Thesis : Photovoltaic Cell Modeling Via Metaheuristic Algorithms

Institute : Istanbul Gelisim University Institute of Graduate Studies

Department : Electrical and Electronics Engineering

Thesis Type : Master

Date of the Thesis : 21.11.2022

Page Number : 59

Thesis Supervisor : Assoc. Prof. Dr. Indrit MYDERRIZI

Index Terms : Genetik Algoritmalar, Corona virüs sürü bağışıklığı optimizasyonu, fotovoltaik hücre parametreleri tahmini, parametre çıkarma

Turkish Abstract : Bu tez, yakıt yanmasından kaynaklanan kayıpları belgeleyen uluslararası kuruluşlardan alınan veriler eşliğinde fosil yakıtlara güvenmenin olumsuz etkilerini ortaya koyacaktır. Daha sonra, sürdürülebilir bir ikame olarak güneş enerjisine odaklanılarak ve mevcut durumda yaygın olarak kullanılan karbon bazlı yakıtların yerini almak için neden yetersiz olduğuna dair bir açıklama ile ortak yenilenebilir enerji kaynakları listelenir.

Distribution List : 1. To the Institute of Graduate Studies of Istanbul Gelisim University
2. To the National Thesis Center of YÖK (Higher Education Council)

Ahmed AZEEZ

**REPUBLIC OF TURKEY
ISTANBUL GELISIM UNIVERSITY
INSTITUTE OF GRADUATE STUDIES**

Department of Electrical and Electronics Engineering

**PHOTOVOLTAIC CELL MODELING VIA
METAHEURISTIC ALGORITHMS**

Master Thesis

Ahmed Raed Azeez AZEEZ

Supervisor

Assoc.Prof.Dr. Indrit MYDERRIZI

Istanbul – 2022

DECLARATION

I hereby declare that in the preparation of this thesis, scientific and ethical rules have been followed, the works of other persons have been referenced in accordance with the scientific norms if used, there is no falsification in the used data, any part of the thesis has not been submitted to this university or any other university as another thesis.

Ahmed AZEEZ

.../.../2022



TO ISTANBUL GELISIM UNIVERSITY
THE DIRECTORATE OF GRADUATE EDUCATION INSTITUTE

The thesis study of Ahmed Raed Azeez AZEEZ titled as Photovoltaic Cell Modeling Via Genetic Algorithms has been accepted as MASTER in the department of Electrical-Electronics Engineering by out jury.

Director

Assoc. Prof. Dr. Indrit MYDERRIZI

(Supervisor)

Member

Asst. Prof. Dr. Serkan GONEN

Member

Asst. Prof. Dr. A.F.M. Shahan SHAH

APPROVAL

I approve that the signatures above signatures belong to the aforementioned faculty members.

... / ... / 20..

Prof. Dr. Izzet GUMUS

Director of the Institute

SUMMARY

This thesis will exhibit the adverse effects of relying on fossil fuels, accompanied by data from international organizations documenting losses inflicted by fuel combustion. The common renewable energy sources are then listed, with a focus on solar as a sustainable substitute and an explanation of why it is in its current state insufficient to replace commonly used carbon-based fuels.

The methods and technologies used to mend solar energy drawbacks will be mentioned; then light will be shed on Genetic Algorithm Optimization as a form of an overview containing essential facts and information regarding GAs alongside mentioning notable studies that have used various types of GAs to model Photovoltaic Cells.

Next, the mathematical modeling for PV cells will be introduced alongside their equivalent circuits, topologies, and equations. The burdens that held PV cells back will be clarified. PV cell parameters estimation methods will be justified to solve some of the difficulties facing solar energy, specifically metaheuristics, with its vast catalog of optimization algorithms.

Afterward, the Coronavirus Herd Immunity Optimization algorithm will be presented, along with its inspiration circumstances. The algorithm procedure will be explained by listing all its steps in the form of text, chart, and Pseudocode. Concluding with use case scenarios and behavioral analysis of the algorithm.

Following that, three of the most popular photovoltaic cell models' data will be used to test the viability of coronavirus herd immunity optimization to extract unknown photovoltaic parameters; the properties of these cells will be detailed with respect to the circumstantial elements at the time their data was captured.

The methodology for obtaining the results will be listed in detail. The extracted PV cell parameters will be listed and graphed, then analyzed and compared to parameters

extracted by other state-of-the-art meta-heuristic optimization algorithms which have been used in literature.

The final judgment of the findings will then be made, along with the criteria that were chosen, and will be followed by a recommendation for future work to further enhance the outcomes or to broaden the scope of the used algorithm.

Keywords: Genetic Algorithms, Corona virus herd immunity optimization, photovoltaic cell parameters estimation, parameters extraction



ÖZET

Bu tez, yakıt yanmasından kaynaklanan kayıpları belgeleyen uluslararası kuruluşlardan alınan veriler eşliğinde fosil yakıtlara güvenmenin olumsuz etkilerini ortaya koyacaktır. Daha sonra, sürdürülebilir bir ikame olarak güneş enerjisine odaklanılarak ve mevcut durumunda yaygın olarak kullanılan karbon bazlı yakıtların yerini almak için neden yetersiz olduğuna dair bir açıklama ile ortak yenilenebilir enerji kaynakları listelenir.

Güneş enerjisinin dezavantajlarını gidermek için kullanılan yöntem ve teknolojilerden bahsedilecektir; Daha sonra, Fotovoltaik Hücreleri modellemek için çeşitli GA'ları kullanan önemli çalışmalardan bahsetmenin yanı sıra GA'larla ilgili temel gerçekleri ve bilgileri içeren bir genel bakış biçimi olarak Genetik Algoritma Optimizasyonuna ışık tutulacaktır.

Daha sonra, eşdeğer devreler, topolojiler ve denklemlerle birlikte PV hücreleri için matematiksel modelleme tanıtılacaktır. PV hücrelerini geride tutan yükler açıklığa kavuşturulacaktır. PV hücre parametreleri tahmin yöntemleri, geniş optimizasyon algoritmaları kataloğu ile güneş enerjisinin, özellikle meta-sezgisellerin karşılaştığı bazı zorlukları çözmek için gereçlendirilecektir.

Daha sonra Coronavirüs Sürü Bağışıklığı Optimizasyonu algoritması ilham koşulları ile birlikte sunulacaktır. Algoritma prosedürü, tüm adımları metin, grafik ve Pseudocode şeklinde listelenerek açıklanacaktır. Kullanım senaryoları ve algoritmanın davranışsal analizi ile sonuçlanmaktadır.

Bunu takiben, bilinmeyen fotovoltaik parametreleri çıkarmak için koronavirüs sürü bağışıklığı optimizasyonunun canlılığını test etmek için en popüler fotovoltaik hücre modellerinden üçü kullanılacak; bu hücrelerin özellikleri, verilerinin alındığı andaki durumsal unsurlara göre detaylandırılacaktır.

Sonuçları elde etme metodolojisi ayrıntılı olarak listelenecektir. Çıkarılan PV hücre parametreleri listelenecek ve grafiklendirilecek, daha sonra analiz edilecek ve literatürde kullanılan diğer son teknoloji meta-sezgisel optimizasyon algoritmaları tarafından çıkarılan parametrelerle karşılaştırılacaktır.

Daha sonra, seilen kriterlerle birlikte bulguların nihai kararı verilecek ve bunu, sonuçları daha da geliřtirmek veya kullanılan algoritmanın kapsamını geniřletmek iin gelecekteki alıřmalar iin bir tavsiye izleyecektir.

Anahtar Kelimeler : Genetik Algoritmalar, Corona virüs sürü baėıřıklığı optimizasyonu, fotovoltaiik hücre parametreleri tahmini, parametre ıkarma



TABLE OF CONTENTS

SUMMARY	i
ÖZET	iii
TABLE OF CONTENTS	v
ABBREVIATIONS	vi
LIST OF TABLES	ix
LIST OF FIGURES	x
PREFACE	xi
INTRODUCTION	1
PROBLEM STATEMENT	3
SCOPE	3
RELATED WORKS	4

CHAPTER ONE

PV CELLS MODULE MODELING

1.1. Mathematical Modeling and Equivalent Circuit.....	6
--	---

CHAPTER TWO

CORONAVIRUS HERD IMMUNITY OPTIMIZER (CHIO)

2.1. Algorithm inspiration.....	10
2.2. Algorithm Procedure	11
2.3. Algorithm Use Case Scenarios	16
2.4. Application for PV Cell Parameter Estimation	18

CHAPTER THREE

SIMULATION & OUTCOMES

3.1. Simulation.....	19
3.2. Test Subject PV Cells	19
3.3. Results	20
3.4. Statistical Analysis.....	31
3.5. Performance and Runtime	33
3.6. Literature Algorithms	34
3.7. Statistical Analysis.....	36
CONCLUSION AND RECOMMENDATIONS	39
REFERENCES	40

ABBREVIATIONS

WHO	:	World Health Organization
AI	:	Artificial Intelligence
NN	:	Neural Networks
GA	:	Genetic Algorithms
PV	:	Photovoltaic
CHIO	:	Corona Virus Herd Immunity Optimizer
HCPV	:	High Concentrating Photovoltaic
I_{ph}	:	Photocurrent
R_s	:	Series Resistance
R_{sh}	:	Shunt Resistance
SDM	:	Single Diode Model
DDM	:	Double Diode Model
TDM	:	Triple Diode Model
KCL	:	Kirchhoff's Current Law
I_L	:	The Load Current
I_D	:	The Diode Current
I_{sh}	:	The Shunt Current
I_{SD}	:	The Diode's Reverse Saturation Current
q	:	The Electron Charge
I_{ph}	:	Photocurrent
R_s	:	Series Resistance
R_{sh}	:	Shunt Resistance
V_L	:	The Load Voltage

n	:	The Ideality Factor
k	:	Boltzmann's Constant
T	:	The Cells Temperature (K)
I_{D1}	:	Diode 1's Current
I_{D2}	:	Diode 2's Current
$n1$:	The Ideality Factor for Diode 1
$n2$:	The Ideality Factor for Diode 2
I_{SD1}	:	The Reverse Saturation Current for Diode 1
I_{SD2}	:	The Reverse Saturation Current for Diode 2
2019-nCoV:		The Novel Corona Virus
COVID-19:		Corona Virus Disease
$f(x)$:	The Immunity Rate
x	:	The Decision Variable (or Gene)
ub	:	The Upper Bound
lb	:	The Lower Bound
C_0	:	The Initial Infection Count
Max_Itr	:	The Maximum Iterations
HIS	:	Total Population Count
n	:	The Equation Dimensions
BRR	:	Basic Reproduction Rate
Max_{Age} :		Maximum Age
HIP	:	Population Matrix
j	:	Matrix Row
S	:	the Status Vector

$C(x_i^j(t))$:	Infected Gene
$N(x_i^j(t))$:	Susceptible Gene
$R(x_i^j(t))$:	Immune Gene
r	:	Random Value
A_j	:	The Age Vector
EF	:	The Error Factor
RMSE:		The Root Mean Square Error
GPU :		Graphics Processing Unit
FPA :		The Flower Pollination Algorithm
COA :		The Chaotic Optimization Approach
COA :		The Coyote Optimization Algorithm
ICSO :		The Improved Cuckoo Search Optimization
HHO :		Diversification-Enriched Harris Hawks' Optimization
PSOCS	:	Random reselection particle swarm optimization
TPTLBO	:	Triple-Phase Teaching-Learning-Based Optimization
IGWO	:	Grey Wolf Optimizer with Dimension Learning-Based Hunting Search Strategy
WHHO	:	Whippy Harris Hawks Optimization Algorithm

LIST OF TABLES

Table 1: The bounds used in the simulation	20
Table 2: The parameters extracted by CHIO for each PV cell model accompanied by the RMSE.....	21
Table 3: literature algorithms RMSE and their settings compared to CHIO for the Single Diode Model of RTC France PV Cell.	22
Table 4: CHIO algorithm Double Diode Model of the RTC France PV Cell estimated parameters' RMSE and settings listed alongside the other state-of-the-art algorithms.	24
Table 5: Power Watt PWP-201 estimated parameters' RMSE by CHIO followed by the most recent successful algorithms' results RMSE accompanied by their setup specifications.....	31
Table 6: The best, worst, and average RMSE from all the runs of CHIO.....	31
Table 7: The timings are taken from MATLAB for one complete run of CHIO estimating PV cell models' parameters.....	33
Table 8: RMSE of results extracted by CHIO and algorithms used in recent literature.....	34
Table 9: The aggregated RMSE of all CHIO runs followed by the sample of algorithms to benchmark the performance.	37

LIST OF FIGURES

Figure 1: The equivalent circuit of the Single Diode Model.....	7
Figure 2: The equivalent circuit of the Double Diode Model.....	8
Figure 3: The equivalent circuit of the Triple Diode Model.....	9
Figure 4: The Flow Chart For CHIO.....	16
Figure 5: RMSE value over the best run's iterations.....	22
Figure 6: The most optimal run made by CHIO for the RTC France double diode model.....	23
Figure 7: RMSE's convergence rate for the Power Watt PWP-201.....	25
Figure 8: The parameters' values predicted for the SDM of the RTC France solar cell through the iterations.....	26
Figure 9: The seven extracted variables for the RTC France DDM over the iterations of the best CHIO run.....	28
Figure 10: The line charts for the five values produced by CHIO representing the Power Watt PWP-201's properties.....	30
Figure 11: the average RMSE values exerted by CHIO over the total 30 runs made for the RTC France single and double diode models.....	32
Figure 12: The fitness function for the parameters extracted by CHIO for the Power Watt PWP-201 model over the 30 runs.....	33

PREFACE

This work was made possible by God's blessings, unwavering family support, and the Advisors' constant guidance.

Many thanks to Istanbul Gelisim University's opportunity, the outstanding professors, and the staff continually striving to help the students thrive and advance their knowledge.

Last but not least, it was a great honor to live and study in Turkiye, a nation that always gives a fair chance to all beings without any prejudices, treats all of them with equality, and respects their rights.



INTRODUCTION

Fossil fuels are currently the world's number one source of energy, these resources are not going to suffice in the future, they are finite and bound to be depleted(Korpela, 2006). Furthermore, 4.2 million deaths occur worldwide by exposure to ambient air pollution every year, there are 3.8 million deaths caused by household exposure to smoke induced by combustible fuels ,about 90% of humans live in environments exceeding the World Health Organization (WHO) guidelines (World Health statistics 2021: A visual summary, 2021). Therefore, pollution by combustible fuels is not just a hot topic to be trending online or circulated in the media; it is a disaster that keeps worsening each second if not halted by using alternative, environmentally friendly energy sources such as solar and geothermal energy.

The dilemma with green energy sources was always efficiency and cost; it is way less effective than fossil fuels and is very expensive to manufacture. For example, the maximum average efficiency of commercial solar panels is approximately 20%(Zekry vd., 2018), which cannot cover the current or future needs. However, on the brighter side, researchers have found an impressive theoretical improvement in solar panels' efficiency of around 50%(Green vd., 2022).

Many research breakthroughs were achieved by the advancement of computer systems and their software. Artificial Intelligence (AI), Neural Networks (NN), and Genetic Algorithms (GA) are essential for simplifying matters of massive complexity. GAs are Optimization methods that can find optimized solutions for the complicated, non-conventional, and nonlinear types of problems. (Callier & Sandel, 2021; Katoch vd., 2021)

Holland introduced Genetic Algorithms in his book "Adaptation in natural and artificial systems" in 1975. He explained how nature's rules of natural selection could be applied to solve optimization equations. Since then, his creation has evolved to become today's robust optimization and search tool(Sivanandam & Deepa, 2008).

Generally, there are five phases of GAs:

- Initialization
- Fitness Calculation

- Selection
- Crossover
- Mutation

There are four types of GAs(Jenkins vd., 2019):

- Generational GA
- Steady State GA
- Steady-Generational GA
- $(\mu+\mu)$ -GA

As for the inspiration side of creating these algorithms, it could be broadly categorized into:

- Physics-Based Algorithms
- Swarm-Based Algorithms
- Human-Based Algorithms (Bhattacharyya vd., 2020)

Numerous studies have employed optimization algorithms to find the unknown parameters of PV cells, achieving promising results, thus reducing designing costs while increasing efficiency at the same time. These papers will be discussed, and their outcomes will be used as a reference to benchmark the results obtained by this research.

PV cells will be explored in the following sections, and their equivalent circuits will be defined. Subsequently, Corona Virus Herd Immunity Optimizer (CHIO) will be described and utilized to guess the unknown parameters in the equivalent circuit of the PV cells.

PROBLEM STATEMENT

In our ever-expanding world, the need for more energy sources is increasing rapidly. Despite the fact that burnable fuels are a sufficient energy supply, they lack two crucial elements: sustainability and environmental neutrality.

An existential question arises when discussing sustainability: will fossil fuels last indefinitely? The obvious answer is no. Furthermore, the energy demand is continuously increasing.

As for fossil fuels' Environmental neutrality, it is impossible due to the carbon emissions released as a by-product of combustion, which causes severe harm to the planet, and the challenge of mitigating such damage is burdensome and costly.

Enter solar power that solves many of the issues associated with conventional energy sources; however, its high production cost accompanied by its low efficiency compared to fossil fuels hinders its wide adoption.

SCOPE

This thesis aims to advance photovoltaics by extracting the unknown parameters of photovoltaic (PV) cells, which can help alleviate some designing expenses and grow the PV cell competence; the PV cell parameters will be extracted using the Coronavirus Herd Immunity Optimizer. The algorithm has never been tested to date in the PV cell parameters estimation field. Therefore, this thesis will gauge the algorithm's ability and compare its results with other state-of-the-art algorithms used by researchers in the literature in recent years.

RELATED WORKS

Genetic algorithm was used to identify the unknown parameters of PV cells 21 years prior to this work, and it has also studied the effects of varying the temperature for three PV cells (monocrystalline (HIT-215), multi-crystalline (KC200GT), and thin-film (ST40)). The absolute error between the extracted results and the data sheets ranged from 0.009 to 0.016. (Jervase vd., 2001)

Ten years later, Differential Evolution (Ishaque & Salam, 2011) has followed a three-parameter equivalent circuit design of the single diode model for three commercial PV cells (thin-film (ST40), monocrystalline SM55, and multi-crystalline s75).

Improved Adaptive Differential Evolution (Jiang vd., 2013) was employed a while after to produce enhanced results, the new version of Differential Evolution autonomously applies control parameters on the go, which had parameters more desirable than the previous version.

The Flower Pollination Algorithm (Alam vd., 2015) is inspired by plants' propagation methods, where pollen is transferred via insects from one plant to another. The researchers extracted PV cell parameters for the single diode model equivalent circuit of the RTC France and Power Watt PWP-201; the research also included the double diode model equivalent circuit of the RTC France solar cell model. The algorithm has achieved results so impressive; that is still viable to be used seven years after its publishing. However, the hindrances of FPA were converging prematurely, and it is not intuitive to implement.

The Chaotic Optimization Approach (COA) by (Ćalasan vd., 2019) is simple to implement and is not time-consuming; the result came out accurately, at an average of RMSE only slightly lacking in comparison with other algorithms.

Next, The Coyote Optimization Algorithm (COA) (Chin & Salam, 2019) the algorithm is inspired by the social behavior of Coyote packs. The researchers have found very successful results; however, the improved version of COA has more benefits, is faster, and is more stable.

The Improved Cuckoo Search Optimization (ICSO) (Gude & Jana, 2020) followed the reproduction of some cuckoo species and was used to presume the parameters of the single and double diode variants of RTC France solar cell and the single diode model of the Power Watt PWP-201.

Diversification-enriched Harris hawks' optimization with chaotic drifts (HHO) by (Chen, Jiao, Wang, Heidari ve Zhao, 2020), inspired by the hawks' hunting mechanism, where hawks surround the prey from all directions shocking it into awe, like the hawks, the algorithm encompasses the solution by its exploration/exploitation stages till reaching a satisfactory result.

Random reselection particle swarm optimization (PSOCS) by (Fan vd., 2022) Cuckoo Search imitates a bird flock's food-seeking behavior mixed with the particle swarm optimization ability, making it a hybrid algorithm that has pros from both merged algorithms.

Triple-Phase Teaching-Learning-Based Optimization (TPTLBO) by (Liao vd., 2020) the algorithm works similarly to the teaching-learning process used in schools. The researchers have tested it to extract PV cell parameters with remarkably consistent results.

Grey Wolf Optimizer with Dimension Learning-Based Hunting Search Strategy (IGWO) by (Yesilbudak, 2021) is one of the newest modifications of the widely popular algorithm, and it has several upgrades that include a more diverse population of solutions, local optima avoidance strategy, and sound exploration/exploitation balancing ability.

Whippy Harris Hawks Optimization Algorithm (WHHO) by (Naeijian, Rahimnejad, Ebrahimi, Pourmousa ve Gadsden, 2021); is a new modification to the harris hawks' optimization algorithm. It solves some drawbacks of the algorithm by adding a phase at which the worst candidates are terminated, and better ones are added in their place, which has helped the algorithm with its issues of getting stuck into local optima and failing to converge.

CHAPTER ONE

PV CELLS MODULE MODELING

An accurate PV Cell model representation is crucial to analyzing the cell's performance. Therefore, this section will shed light on the modeling methods of PV cells, and the materials PV cells are made-of will be briefly discussed.

The most used material for PV Cell manufacturing is crystalline silicon which can be categorized into three primary forms: thin film, monocrystalline silicon, and multi-crystalline silicon (Ishaque & Salam, 2011).

Also, the high concentrating photovoltaic (HCPV) method has to be mentioned for its effectiveness and low manufacturing costs with the introduction of Fresnel lenses (Mivd., 2016).

1.1. Mathematical Modeling and Equivalent Circuit

The equivalent circuit of a PV cell usually consists of a PV constant current source (I_{ph} , which represents the photocurrent, a series resistance (R_s) that represents materials resistance, and a shunt resistance (R_{sh}) that occurs at the junction of the diode due to electron and hole trapping (Zekry vd., 2018).

Based on the number of parallel diodes in the circuit, PV cells can be divided into three main models: Single Diode Model (SDM) (Moshksar & Ghanbari, 2017), Double Diode Model (DDM) (Humada vd., 2016), and Triple Diode Model (TDM) (Allam vd., 2016; Khanna vd., 2015).

The single diode model shown in figure 1 is the most popular amongst the bunch due to its simplicity and reliability of results. By utilizing Kirchhoff's Current Law (KCL), it can be represented by equation 1:

$$I_L = I_{ph} - I_D - I_{sh} \dots (1)$$

Where I_L denotes the resultant current of the circuit, I_D is the diode current can be found by Shockley's Equation, and I_{sh} stands for the shunt current.

The diode current can be found using the equation below:

$$I_D = I_{SD} \left[\exp \left(\frac{q(V_L + I_L R_S)}{nkT} \right) - 1 \right] \dots (2)$$

Where I_{SD} is the diode's reverse saturation current, q is the electron charge, V_L is the load voltage, n represents the ideality factor, k is Boltzmann's constant, and T is the cell's temperature measured in Kelvin.

Moreover, the shunt current is obtained using equation 3:

$$I_{sh} = \frac{(V_L + I_L R_S)}{R_{sh}} \dots (3)$$

By combining the three previous equations, the total SDM current equals:

$$I_L = I_{ph} - I_{SD} \left[\exp \left(\frac{q(V_L + I_L R_S)}{nkT} \right) - 1 \right] - \frac{(V_L + I_L R_S)}{R_{sh}} \dots (4)$$

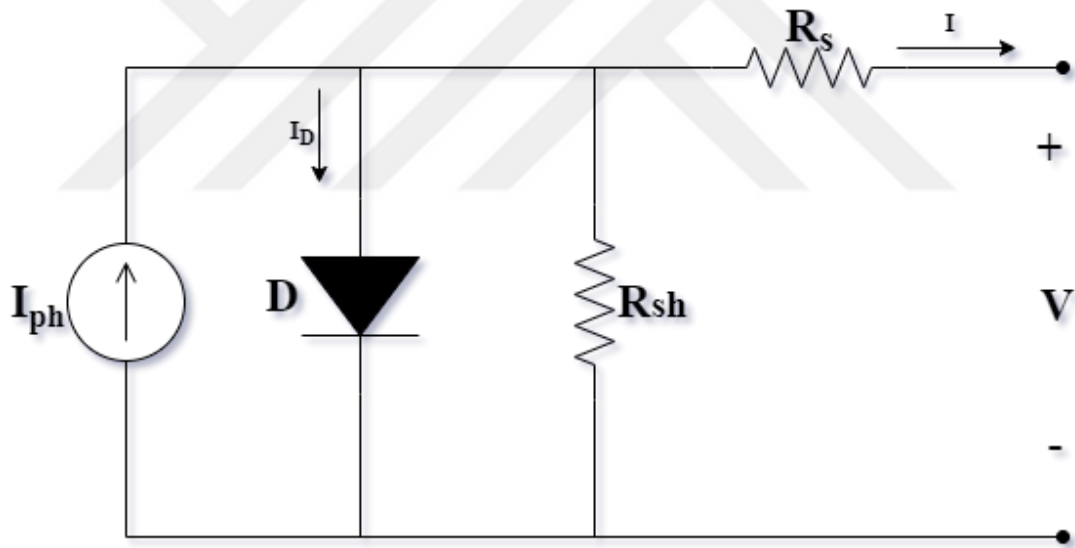


Figure 1:The equivalent circuit of the Single Diode Model.

The second variant is the Double Diode Model, which has two parallel diodes; as the name suggests, the second diode was added to count for the losses caused by the recombination failure in the PN junction (Ishaque, Salam ve Taheri, 2011). Characterized in Figure 2, DDM is also famous for being straightforward and intuitive. Moreover, it can be mathematically described in equation (5) using KCL:

$$I_L = I_{ph} - I_{D1} - I_{D2} - I_{sh} \dots (5)$$

Where I_{D1} and I_{D2} signify the current for diodes 1 and 2 separately. By employing equations (2) and (3), the entire current of the DDM can be found as follows:

$$I_L = I_{ph} - I_{SD1} \left[\exp \left(\frac{q(V_L + I_L R_S)}{n1 k T} \right) - 1 \right] - I_{SD2} \left[\exp \left(\frac{q(V_L + I_L R_S)}{n2 k T} \right) - 1 \right] - \frac{(V_L + I_L R_S)}{R_{sh}} \dots (6)$$

Where I_{SD1} and $n1$ represent the reverse saturation current and ideality factor for the first diode, respectively. As for the second diode I_{SD2} and $n2$ will also represent the reverse saturation current and ideality factor correspondingly.

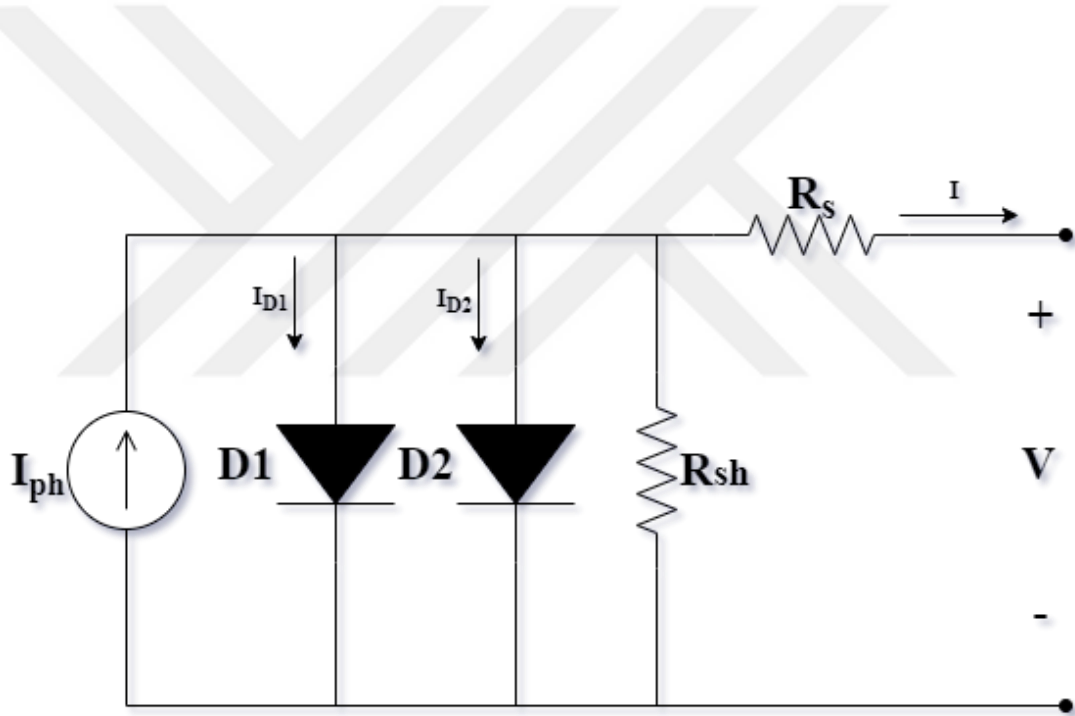


Figure 2: The equivalent circuit of the Double Diode Model.

The last model presented in figure 3 differs from the others for its complex nature, as seen in its mathematic equation (induced by: $I_L = I_{ph} - I_{D1} - I_{D2} - I_{D3} - I_{sh}$) below, and its behavior is more challenging to predict; therefore, it will not be used in this thesis to assure reliability and consistent outcomes.

$$I_L = I_{ph} - I_{SD1} \left[\exp \left(\frac{q(V_L + I_L R_S)}{n_1 k T} \right) - 1 \right] - I_{SD2} \left[\exp \left(\frac{q(V_L + I_L R_S)}{n_2 k T} \right) - 1 \right] - I_{SD3} \left[\exp \left(\frac{q(V_L + I_L R_S)}{n_3 k T} \right) - 1 \right] - \frac{(V_L + I_L R_S)}{R_{sh}} \dots (7)$$

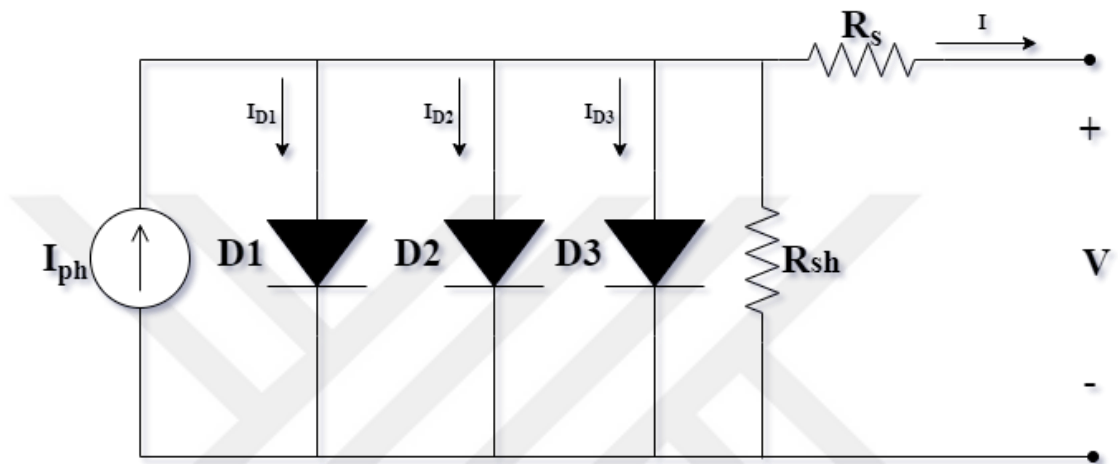


Figure 3: The equivalent circuit of the Triple Diode Model.

CHAPTER TWO

CORONAVIRUS HERD IMMUNITY OPTIMIZER (CHIO)

In August 2020, a research paper was published (Al-Betar vd., 2021) announcing a new meta-heuristic algorithm based on humans' herd immunity concept as a method to combat the COVID-19 pandemic.

2.1. Algorithm inspiration

Viruses usually spread rapidly amongst the population; most viruses also evolve to spread faster, more incognito, thus affecting their victims with more severity.

To combat the spread of viruses, health providers usually treat the infected cases and keep them and their contacts in quarantine conditions. Herd immunity must be achieved to avoid the pandemic, either by vaccination or recovery of infected cases.

Wuhan, 2019, The Novel Corona Virus (2019-nCoV) started its spread through the globe; the World Health Organization named the new disease COVID-19.

Herd immunity is a term used for a population with a sizeable immune group (either by vaccination or by recovery from infection); thus, the disease's spread will be hindered. The exact threshold should be 60%, immune members.

Social distancing is the void that must be held between humans to avoid the transfer of the disease; this distance has been set at 1.8 meters.

An individual that is not infected or immune is denoted as susceptible. Once infected, the individual becomes a transmitter of the disease based on several factors; there will be two possible outcomes for an infected case the first one is being recovered, and the second one happens to be, unfortunately, dead.

As indicated by researchers, there are three primary levels to achieving herd immunity:

- a large proportion of the population gets infected and transfers the disease to another large portion of the population.

- Most cases are recovered, whereas the remaining minority does not survive.
- After some time, most of the population would have immunity from the disease.(Al-Betar vd., 2021)

2.2. Algorithm Procedure

The algorithm follows the strategy of herd immunity; the flowchart in figure 4 represents its procedures; it has six core steps:

Step 1: Initialization

Initialization of the algorithm parameters and the optimization equation: in this step, the problem to be optimized is transformed into an objective function as follows:

$$\min_x f(x) \quad x \in [ub, lb] \dots (8)$$

where $f(x)$ is the immunity rate, x is the decision variable (or Gene) indexed by i , and n which represents the entirety of genes; the value for each gene value ranges from lb_i to ub_i .

CHIO has four algorithmic parameters:

- C_0 : representing the initial infection count that usually starts with one.
- Max_Itr stands for the maximum allowed iterations.
- HIS: a number denoting the total population count.
- n : the equation dimensions.

Additionally, CHIO has two control parameters:

- BRR : basic reproduction rate.
- Max_{Age} : maximum age at which the case must be determined as recovered or dead.

Step 2: Population Generation

The startup population of the herd immunity is created heuristically; the quantity of the population, as mentioned earlier, is defined by HIS . The resultant genes are stored in a two-dimensional matrix denoted by HIP .

$$HIP = \begin{bmatrix} x_1^1 & x_2^1 & x_n^1 \\ x_1^2 & x_2^2 & x_n^2 \\ x_n^{HIS} & x_n^{HIS} & x_n^{HIS} \end{bmatrix} \quad \dots (9)$$

Each row j represents an individual gene x^j that is created by the following:

$$x_i^j = lb_i + (ub_i - lb_i) * U(0,1) \quad \dots (10)$$

$$\forall i, 1, 2, \dots, n. \forall j = 1, 2, \dots, HIS.$$

The immunity rate is determined using equation (8); the status vector (S) is capped by HIS length and can be used as a reference to indicate each case status in HIP (0 for a susceptible case or 1 for an infected case) (S) is initialized randomly with the length value identical to Co .

Step 3: Gene Evolution

This is the primary gene transformation loop in $CHIO$; each gene will either remain untouched or will be affected by social distancing and according to the percentage of BRr where:

$$x_i^j(t+1) \leftarrow \begin{cases} x_i^j(t) & r \geq BRr \\ C(x_i^j(t)) & r < \frac{1}{3}BRr \quad // \text{infected} \\ N(x_i^j(t)) & r < \frac{2}{3}BRr \quad // \text{susceptible} \\ R(x_i^j(t)) & r < BRr \quad // \text{immuned} \end{cases} \quad \dots (11)$$

The value of r is a random value that ranges from 0 to 1

For an infected case, the new gene will be calculated as follows:

$$C(x_i^j(t)) = x_i^j(t) + r * (x_i^j(t) - x_i^c(t)) \quad \dots (12)$$

Note that (x_i^c) is chosen heuristically from within the infected cases indicated by the status vector (S) where:

$$c = \{i | S_i = 1\} \quad \dots (13)$$

For a susceptible case, the gene will be replaced according to equation (14):

$$N(x_i^j(t)) = x_i^j(t) + r * (x_i^j(t) - x_i^m(t)) \quad \dots (14)$$

Where $x_i^m(t)$ is chosen at random from the susceptible genes marked by (S) such as:

$$m = \{i | S_i = 0\} \quad \dots (15)$$

Lastly, for an immune case, the gene will be updated as follows:

$$R(x_i^j(t)) = x_i^j(t) + r * (x_i^j(t) - x_i^v(t)) \quad \dots (16)$$

$x_i^v(t)$ is chosen from within any of the cases indicated as immune by (S) and can be represented by:

$$f(x^v) = \arg \min_{j \sim \{k | S_k = 2\}} f(x^j) \quad \dots (17)$$

Step 4: Population Update

In this step, the gene population will be updated; each case will be evaluated and changed into a new value if the new value is improved. In addition, in case of an update, the age A_j and status S_j vectors will be updated by increasing the age vector by one if the status vector S_j value was one.

Step 5: Gene Termination

If a gene becomes stagnant for some iterations and its current value is not within the desired outcome, it will be terminated (dead case), and a new gene will be generated using equation (10); both S_i and A_j it will be set to zero. This process is crucial to vary the population and avoid having a local optima.

Step 6: Halt Criteria

The algorithm will loop steps three to six until reaching a termination condition, usually achieving the predetermined maximum number of iterations. After the termination, the gene population should split between susceptible and immune cases and has an absence of infected cases.

The following text represents CHIO Pseudocode:

- **Step 1: Initialize CHIO parameters**

Appoint values to (*HIS*, *Sr*, and *MaxAge*).

- **Step 2: Generate Herd-Immunity Population**

$$x_i^j = lb_i + (ub_i - lb_i) * U(0,1), \forall i = 1, 2, \dots, n, \text{ and } \forall j = 1, 2, \dots, HIS.$$

Calculate the fitness of each search agent

Set $S_j = 0 \forall j = 1, 2, \dots, HIS$.

Set $A_j = 0 \forall j = 1, 2, \dots, HIS$.

- **Step 3: Herd immunity evolution**

while ($t \leq Max\ itr$) do

for $j = 1$ to HIS do

is Corona ($x_j(t + 1) = false$)

for $i = 1$ to N do

if ($r < \frac{1}{3}BRr$) then

$$x_i^j(t+1) = C(x_i^j(t)) \text{ Eq. (12)}$$

is Corona ($x_j(t + 1) = true$)

else if ($r < \frac{2}{3}BRr$) then

$$x_i^j(t+1) = N(x_i^j(t)) \text{ Eq. (14)}$$

else if ($r < BRr$) then

$$x_i^j(t+1) = R(x_i^j(t)) \text{ Eq. (16)}$$

else

$$x_i^j(t+1) = x_i^j(t)$$

end if

end for

- **Step 4: Update herd immunity population**

if ($f(x_j(t + 1)) \leq f(x_j(t))$) then

$x_j(t) = x'_j(t + 1)$

else

$A_j = A_j + 1$

end if

if $f(x_j(t + 1)) < \frac{f(x)^j(t+1)}{\Delta f(x)} \wedge S_j = 0 \wedge is\ Corona(x_j(t + 1))$ then

$S_j = 1$

$A_j = 1$

end if

if $f(x_j(t + 1)) > \frac{f(x)^j(t+1)}{\Delta f(x)} \wedge S_j = 1$ then

$S_j = 2$

$A_j = 0$

end if

- **Step 5: Fatality condition**

if $((A_j \geq MaxAge) \wedge (S_j == 1))$ then

$x_i^j = lb_i + (ub_i - lb_i) * U(0,1), \forall i = 1, 2, \dots, N.$

$S_j = 0$

$A_j = 0$

end if

end for

$t = t + 1$

end while

Here lies the end of the CHIO's Pseudocode; the flow chart below illustrates the abovementioned steps in visually represented details.(Al-Betar vd., 2021)

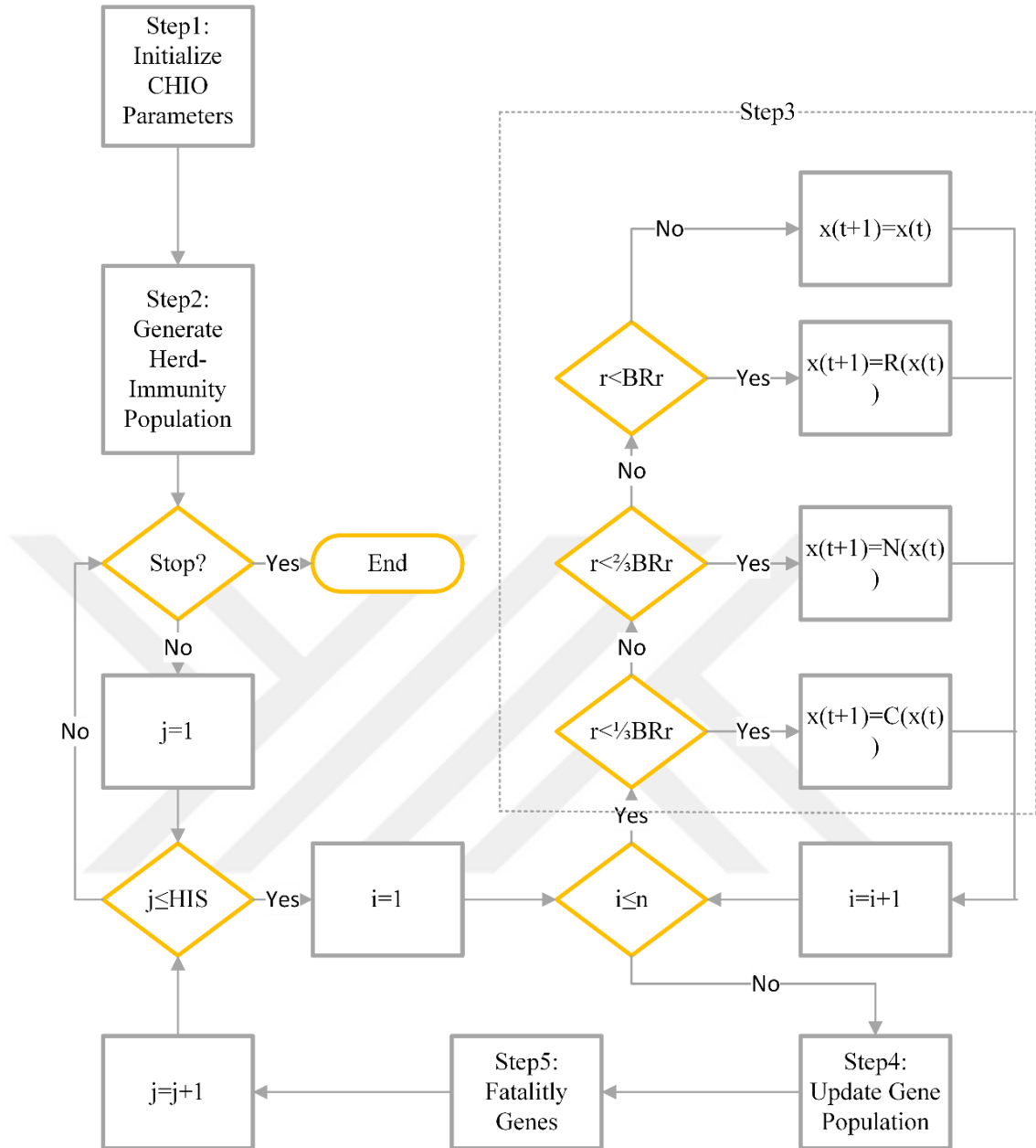


Figure 4:The Flow Chart For CHIO

2.3. Algorithm Use Case Scenarios

The newfound algorithm was used to optimize a very significant number of functions, whether by the creators or other researchers; in this section, the spotlight will be focused on the algorithm’s creators’ tests. Some of these functions were unimodal (with one optimum) to test the algorithm’s exploitation ability. In contrast, others were multimodal (with multiple optimums) to gauge CHIO’s exploration

ability; the sphere function, Rosebrock function, Ackley function, Branin function, and Hartman function are some of the examples used by the introductory paper for CHIO.

It should be noted that basic reproduction rate BRr , and maximum age $MAXage$ are the two control parameters for CHIO, where BRr decides the proportion of the population that gets hit by the pandemic, and, $MAXage$ overlooks the number of iterations the candidate solution remains constant in value before it gets replaced by another.

With all that said, the overall number of equations used to test the ability of the newfound algorithm was 23, and each test was run 30 times. It was noticed that increasing the BRr has caused an increase in the algorithm's ruggedness which induced a better average of results due to increasing the exploration ability, although that required more processing time; On the other hand, decreasing the BRr has caused a faster convergence rate but decreased the algorithm's exploration ability.

As for $MAXage$, it affects CHIO's exploration if changed, theoretically, but after concluding all the test runs, the algorithm creators did not notice an improvement to both the best and average results, thus recommended not changing the default value of 100 for the control parameter.

After finalizing the control parameters, it is important to discuss social distancing principles, where it identifies each of the candidates with three possible statuses: immune (cannot be infected), susceptible (could be infected), and infected. Testers have used three different social distancing strategies:

- Random-random-random, where the new solution is varied by the value of the difference between the current and a random variable for all types of intrans.
- Random-random-best, here the immune candidate gets updated with a value equal to the difference between the current and the best solution, while the other two types of candidates have a change amounted to the difference between the present solution and a random value.
- Random-best-random, in this strategy, the susceptible case is changed according to the value of the variance between the current and the best available solution, while the other two variants of candidates update to a new

value that is amounted to the difference between the instant result and a random value.

- Random-best-best, the last strategy suggested that the infected case's new value would be the alteration between the current candidate and a randomized entry while the remaining cases have their new value changed by the amount of difference between the existing solution and the best output.

based on 30 repetitions of the algorithm for each strategy, it was determined that the first strategy (random- random- random) had induced the best possible results, proving that the stochastic approach has resulted in an improved convergence in general.(Al-Betar vd., 2021)

2.4. Application for PV Cell Parameter Estimation

The CHIO algorithm will be utilized to find the unknown parameters for the PV Cell equivalent circuit.

CHIO's results will be compared to actual extracted results and with results predicted by numerous algorithms studied in the literature, thus verifying the reliability of CHIO's results.

For the single diode model, the following equation, which is derived from equations 1, 2,3, and 4, represents the error function:

$$EF = I_{ph} - I_{SD} \left[\exp \left(\frac{q(V_L + I_L R_S)}{nkT} \right) - 1 \right] - \frac{(V_L + I_L R_S)}{R_{sh}} - I_L \dots (18)$$

For the double diode model, the error function listed below was taken from equations 5 and 6:

$$EF = I_{ph} - I_{SD1} \left[\exp \left(\frac{q(V_L + I_L R_S)}{n1kT} \right) - 1 \right] - I_{SD2} \left[\exp \left(\frac{q(V_L + I_L R_S)}{n2kT} \right) - 1 \right] - \frac{(V_L + I_L R_S)}{R_{sh}} - I_L \dots (19)$$

As for the root mean square error for both models:

$$RMSE = \sqrt{\frac{1}{k} \sum_{i=1}^k (Ef)^2} \dots (20)$$

CHAPTER THREE

SIMULATION & OUTCOMES

3.1. Simulation

In this chapter, to test the viability of CHIO, three PV cell model parameters were extracted: RTC France (single and double diode models) and the Power Watt PWP-20; these specific models were chosen due to their popularity among the papers published in the field of study.

CHIO will be utilized to extract the five unknown parameters (I_{ph} , I_{sd} , R_s , R_{sh} , and a) of the RTC France (Single Diode model and the Power Watt PWP-201 PV cells), as for the double diode model of the RTC France solar cell the unknown parameters are (I_{ph} , I_{sd1} , I_{sd2} , R_s , R_{sh} , a_1 and a_2).

The results were acquired using a laptop computer made by Lenovo, with an AMD Ryzen 7 4000 series processor, 16 GB of RAM, and an Nvidia RTX 2060 GPU. The main software used was MATLAB (2018 Version), installed on a Windows 10 64-bit operating system.

3.2. Test Subject PV Cells

The PV cell models that will be worked on are well trusted in the science community and used as a standard in numerous research projects. The data numbers are provided by (Easwarakhanthan vd., 1986)

RTC France PV cell is a 57mm diameter silicone, and its data was measured at the temperature of (33° Celsius) with an irradiance of (1000 W/m²); this PV cell's parameters are going to be extracted for both the single and double diode models.

Additionally, the Power Watt PWP-201 PV cell is a Polycrystalline Silicone; its known variables were taken at an irradiance of (1000 W/m²), and the temperature of the measurement environment was (45° Celsius), and this model consists of 36 series-connected cells, the single diode model equation will be utilized to obtain the unknown parameters.

3.3. Results

The CHIO algorithm was run multiple times with various setting combinations; the reason was to ensure that the algorithm’s final run was done using the most appropriate settings, giving the algorithm a chance to extract the best possible results. In addition, limits have been set for each extracted parameter to limit the algorithm from deviating; these limits are identical to the limits set by the works used in the comparison section, thus ensuring fairness and accuracy—these bounds are listed in Table 1 below.

Table 1: The bounds used in the simulation

Parameter	RTC France		PowerWatt PWP-201	
	SDM	DDM	SDM	
	Lower Bound	Upper Bound	Lower Bound	Upper Bound
I_{ph} (A)	0	1	0	2
I_{sd}, I_{sd1}, I_{sd2} (μA)	0	1	0	50
R_s (Ω)	0	0.5	0	2
R_{sh} (Ω)	0	100	0	2000
n, n_1, n_2	1	2	1	50

Each setting combination was run 30 times, and the average RMSE of each variety was recorded; the optimal mix was chosen based on the best average RMSE, as exhibited in table 2.

Table 2: The parameters extracted by CHIO for each PV cell model accompanied by the RMSE

RTC France			
Parameter	SDM	DDM	Power Watt PWP-201
I_{ph} (A)	$7.61 \cdot 10^{-1}$	$7.61 \cdot 10^{-1}$	1.03
I_{sd}, I_{sd1}, I_{sd2} (μA)	$3.06 \cdot 10^{-7}$	$9.33 \cdot 10^{-7}, 9.74 \cdot 10^{-8}$	$3.16 \cdot 10^{-6}$
R_s (Ω)	$3.66 \cdot 10^{-2}$	$3.74 \cdot 10^{-2}$	1.22
R_{sh} (Ω)	52.6	57.6	$1.38 \cdot 10^3$
n, n₁, n₂	1.48	1.81, 1.39	1.34
RMSE	$7.75 \cdot 10^{-4}$	$7.48 \cdot 10^{-4}$	$2.27 \cdot 10^{-3}$

It was observed that for the RTC France Single Diode Model, with four solutions infected with the virus that spread with the rate of 0.1 amongst the population of 25 possible solutions that had a maximum age of 100 at which the desired RMSE $7.75 \cdot 10^{-4}$ (listed in table 3), was reached with 5000 maximum allowed iterations, however, in figure 5 it can be noticed that the convergence rate was very high, the algorithm has made a considerable leap within only 1000 iterations, and that puts CHIO within the top performers reviewed by the literature in terms of convergence speed.

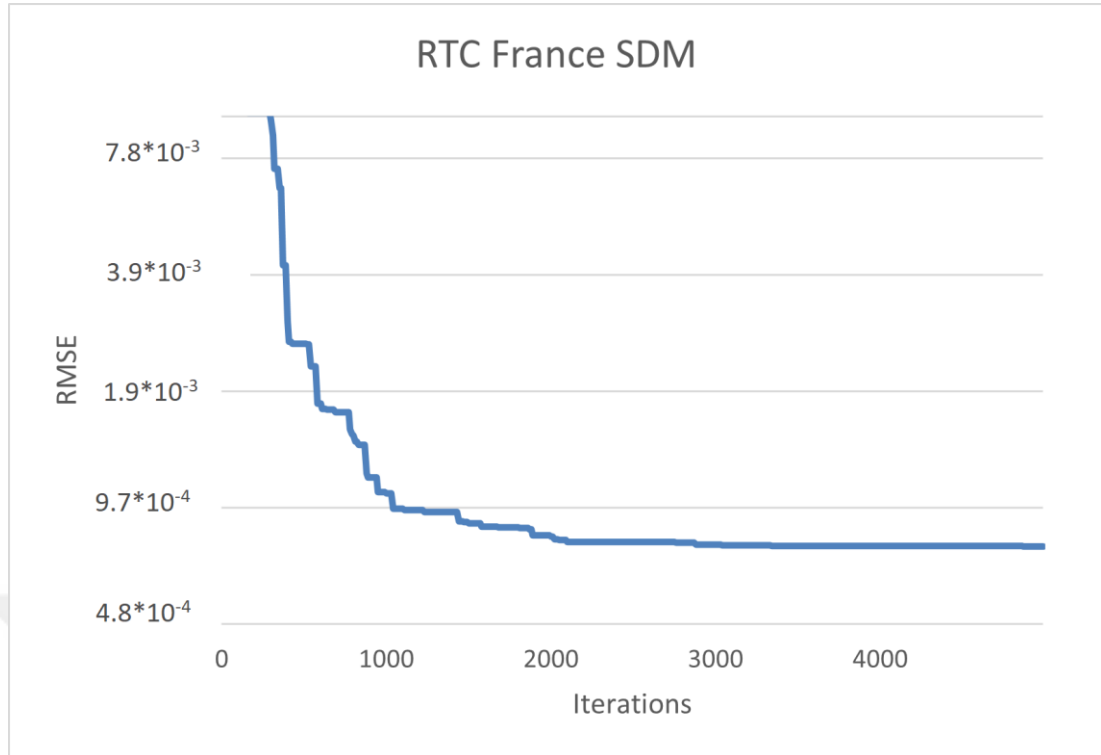


Figure 5: RMSE value over the best run's iterations

Table 3: literature algorithms RMSE and their settings compared to CHIO for the Single Diode Model of RTC France PV Cell.

Method	Population Size	Iterations	Runs
CHIO	25	5000	30
FPA	25	1000	Unspecified
COA ¹	Unspecified	Unspecified	Over 20
COA ²	100	10000	50
ICSO	15	5000	100
HHO	Unspecified	1000	30
PSOCS	10,20,30,40,50,60	12000-14000	20000
TPTLBO	50	-	30

IGWO	15	25000	50
WHHO	30	5000	30

¹ Chaotic Optimization Approach

² Coyote optimization algorithm

Table 3 shows the algorithmic parameters as stated in the respective paper for each algorithm; these settings are usually varied until reaching the combination that will get the best result possible from an optimization algorithm.

As for the Double Diode Model variant, CHIO had one infected candidate at the spreading rate of 0.25 amongst the population of 25 possible solutions permitted to the maximum age of 120; the RMSE was 7.48×10^{-4} (as listed in table 4) with maximum iterations limit set similar to the Single Diode Model at 5000 iterations, nonetheless, figure 6 suggests that the algorithm needed almost fifth the number of iterations to converge towards optimal results.

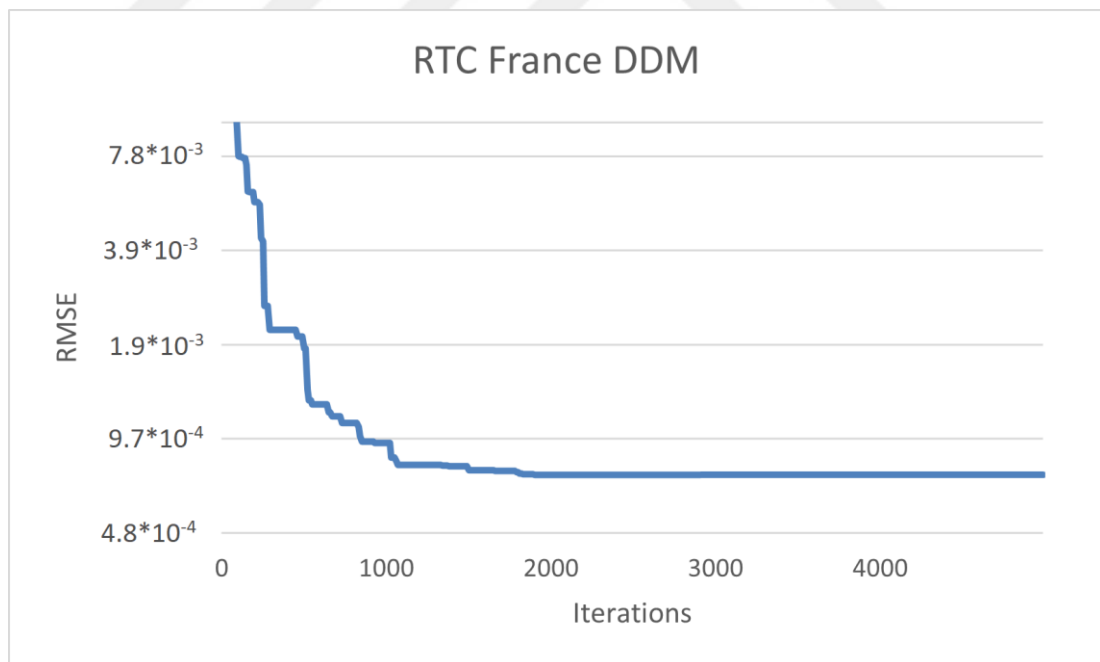


Figure 6: The most optimal run made by CHIO for the RTC France double diode model.

Table 4: CHIO algorithm Double Diode Model of the RTC France PV Cell estimated parameters' RMSE and settings listed alongside the other state-of-the-art algorithms.

Method	Population Size	Iterations	Runs
CHIO	25	5000	30
FPA	25	1000	Unspecified
COA¹	Unspecified	Unspecified	Over 20
COA²	100	10000	50
ICSO	15	5000	100
HHO	Unspecified	1000	30
PSOCS	10,20,30,40,50,60	12000-14000	20000
TPTLBO	50	-	30
IGWO	15	25000	50
WHHO	30	5000	30

¹ Chaotic Optimization Approach

² Coyote optimization algorithm

In the table above, the settings made for each algorithm were very similar, if not even identical, to the algorithmic parameters set for the SDM variant, which confirms the reliability of the algorithms, if the results extracted for the latter model were as optimal as the formal, given that the DDM model has more elements that need to be extracted.

Lastly, the Power Watt PWP-20 had an equal number of infected solutions to the previously mentioned Single Diode; the virus dispersed at the rate of 0.75 midst the 25 possible solutions that had only 10% of the maximum age of the Single Diode Model of the RTC France PV cell, settings in table 5 displays double the number of iterations allowed, due to the model's more challenging parameters limits, which required more intense processing to exert the respectable RMSE of $2.27 \cdot 10^{-3}$ at less than 4000 iterations as seen in figure 7.

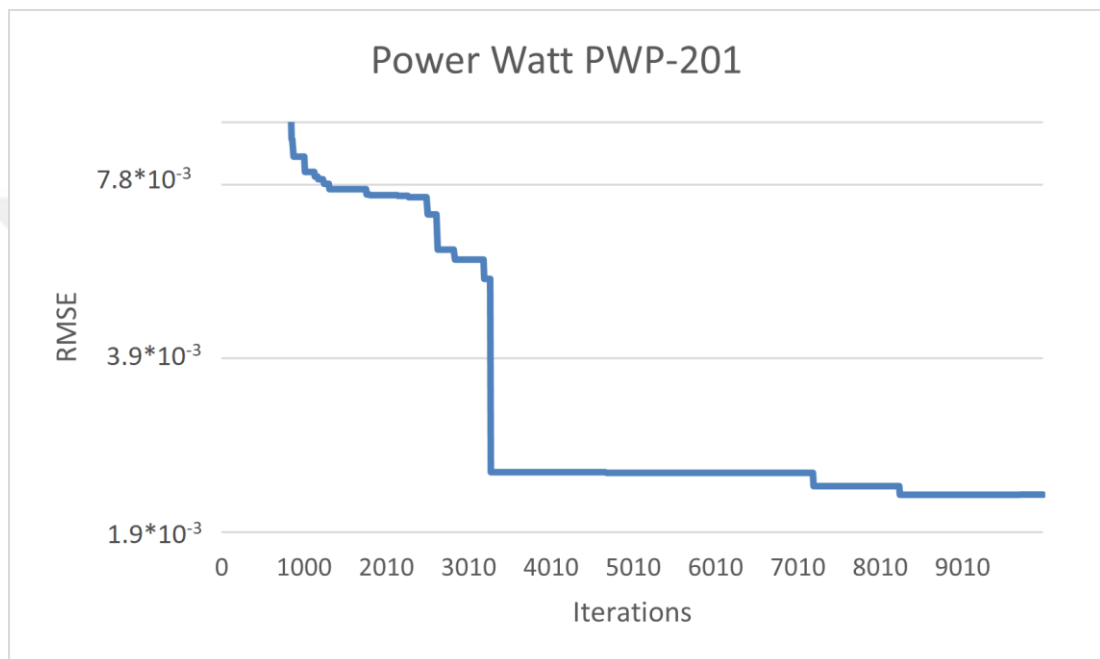


Figure 7: RMSE's convergence rate for the Power Watt PWP-201.

Overall the deep RMSE dives in figures 5,6 and 7 are indications of CHIO's excellent exploitation ability, which is confirmed by the nearly vertical slope dip in the predicted parameters' error fitness function; the same could be said about each predicted parameter's line chart listed in the figures below, it should be noted that the values of each extracted parameter are not supposed to have a decrease in value to be considered successful, unlike the RMSE case, the rating of an optimization algorithm in terms of extracted PV parameters should be measured by the accuracy of the extracted data which can be confirmed by how constant the value is in the iterations that occur beyond the desired results iteration as shown in figures 8, 9, and 10.

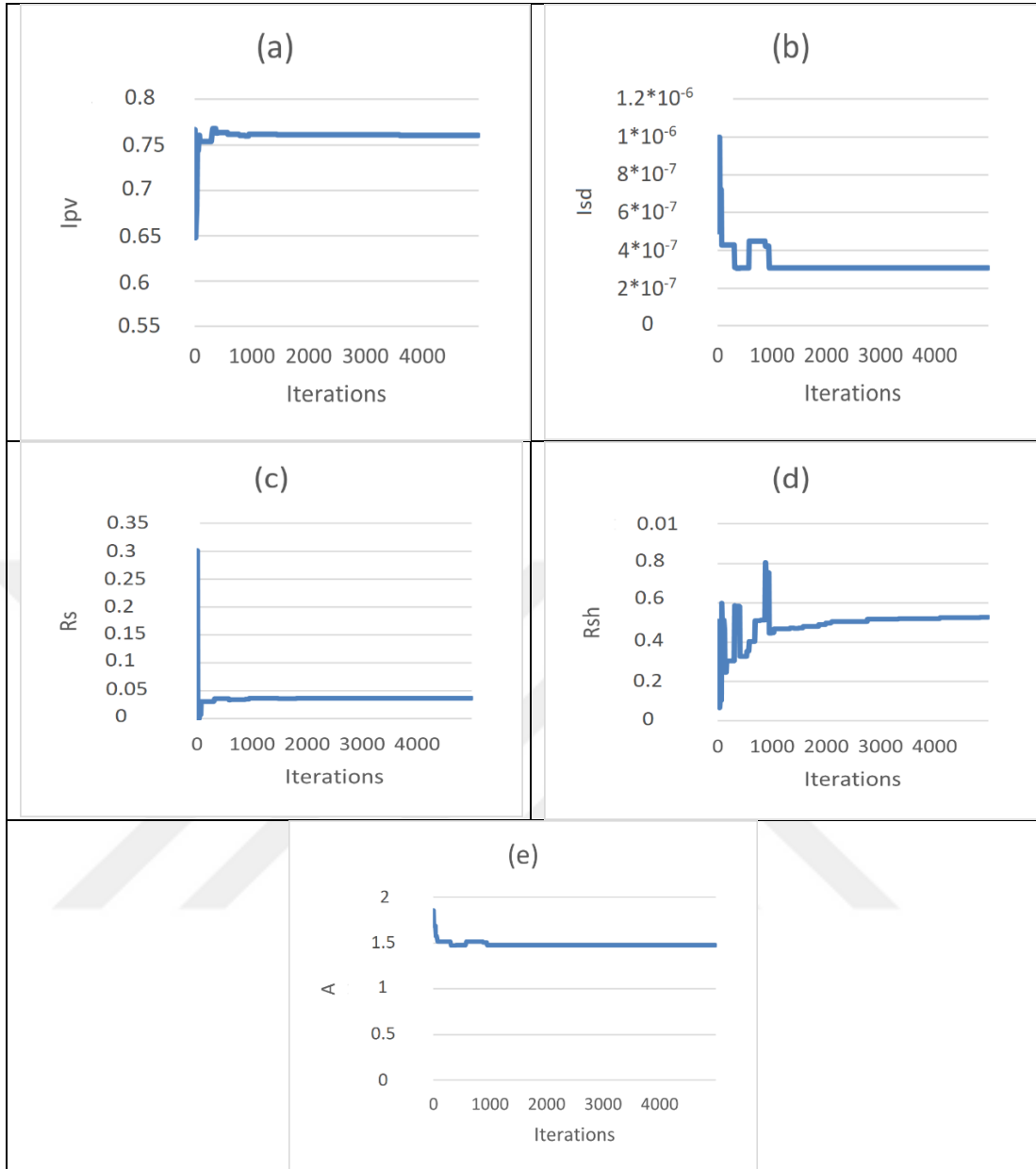


Figure 8: The parameters' values predicted for the SDM of the RTC France solar cell through the iterations.

The figure above illustrates the convergence of each extracted parameter for the RTC France SDM; for the photocurrent, figure 8 (a), CHIO has started in a median position and then explored down value till it hit a stop by the *MAXage* control parameter, returned to the previous level with a few trips exploring options till it reached the desired value within nearly a thousand iterations, kept a steady value till

deciding to study again finding the final result within an additional near one thousand iterations.

As for the I_{sd} value, figure 8 (b) started at a neutral position, took an upwards exploration trip, then dipped back down where it found a better result, and within a few minor ups and downs, found the desired position near the one thousand marker.

The series resistance chart, figure 8 (c), seemed eerily like the I_{pv} 's flipped upside down chart, where the algorithm took an early exploratory jump up high, followed by a deep dive, then returned to the wanted location followed by some minor adjustments and stopped at an iteration not that far from the previous two stops.

The shunt resistance line, figure 8 (d), tells a different story, where CHIO has weaved its way through the candidates back and forth, causing the delay of a few hundred iterations, but that didn't stop it from converging with an impressive two thousand iterations that were followed by little value inflation to reach the optimal resistance.

Finally comes the ideality factor for the diode, figure 8 (e), where the algorithm took a one-way down the value of candidates till reaching the nearly perfect result at less than one thousand iterations.

Next comes the figure showing the results road map for the DDM version of the same model discussed above.

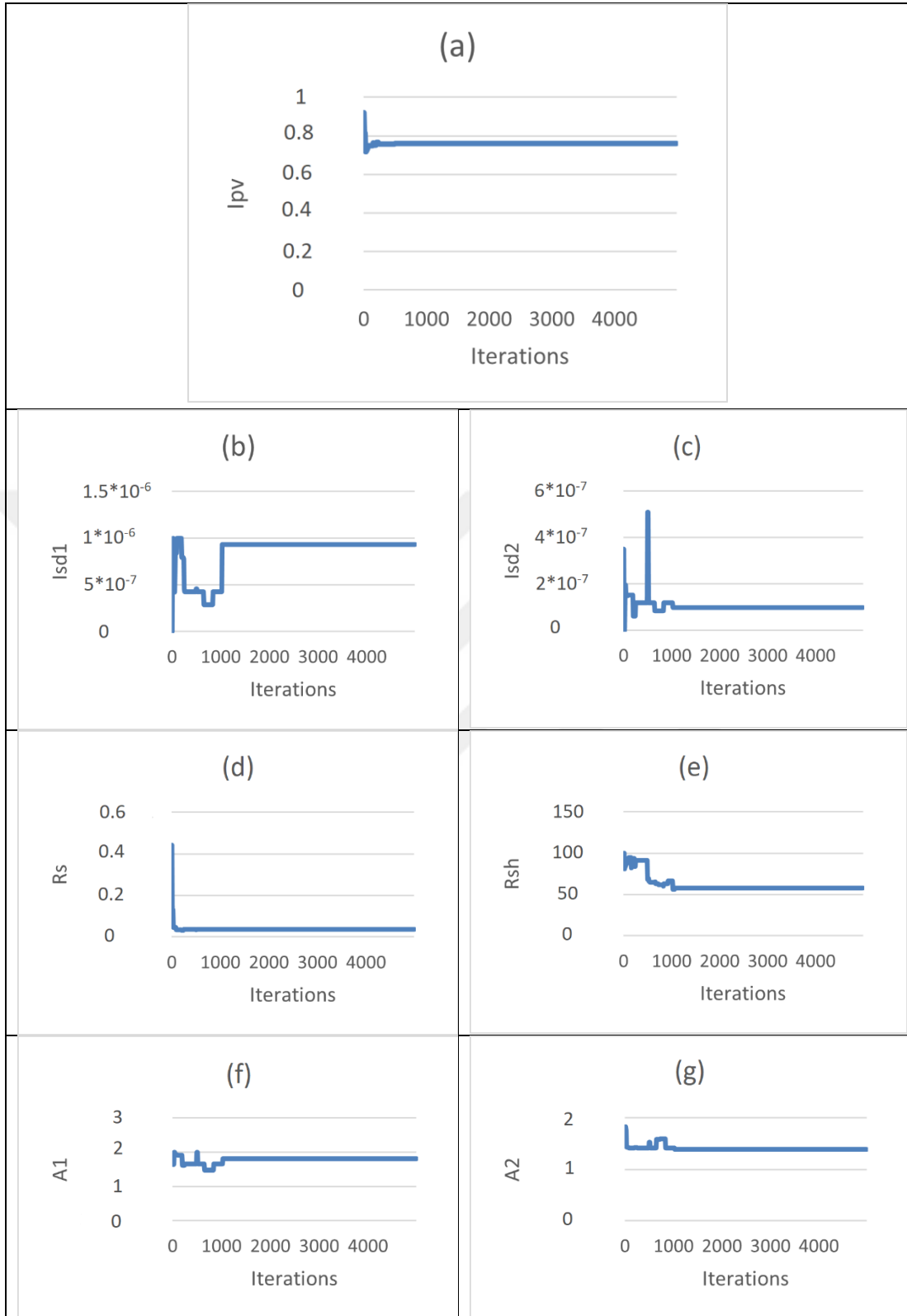


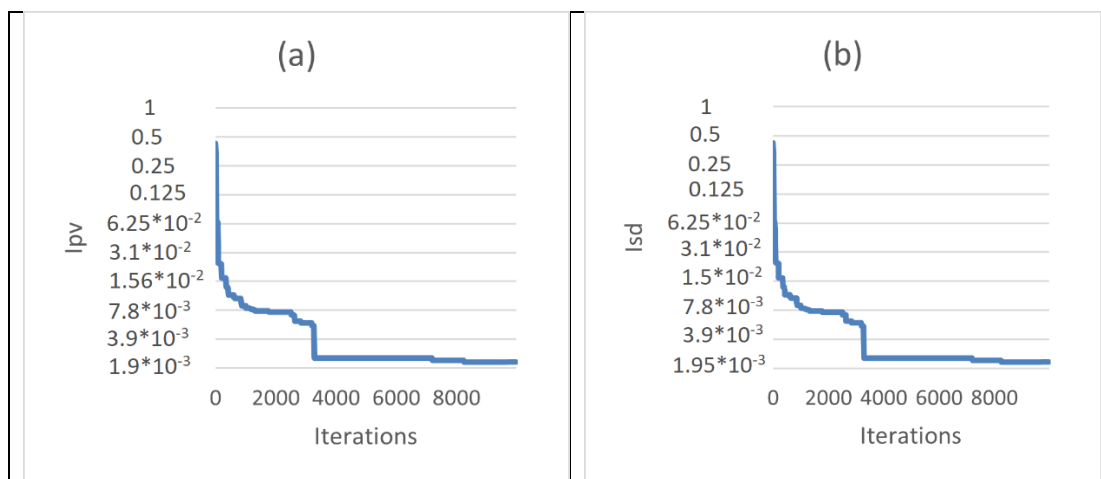
Figure 9: The seven extracted variables for the RTC France DDM over the iterations of the best CHIO run.

In the charts above, it could be noticed that the algorithm has taken one lucky dip for the values of both I_{pv} and R_s , figure 10 (a & e), where it almost immediately found the wanted results.

On the other hand, the algorithm's searching abilities were well tested for the case of both diode currents. For the first one, figure 11 (b), it took several fluctuations up high, then checked the lower values for a while, decided to go back up and accept the near average of the initial exploration ripples. For the second diode, figure 12 (d), the algorithm exhibited a short burst of exploration followed by a massive jump in value that wasn't favorable, forcing CHIO to return to the previous quadrant, then marking the position of the best value available within one thousand tries.

For the shunt resistor, in figure 9 (f), CHIO has scanned within substantial values and slid down to find the right place near the same spot for the parameters mentioned earlier.

Lastly, the algorithm didn't show wild trips for the last two parameters, A_1 and A_2 , figure 13 (g & h); it found the desired results at adjacent positions, with the second ideality factor being found slightly quicker than the first. The following figure shows the very steady CHIO's convergence rate concerning the last PV model.



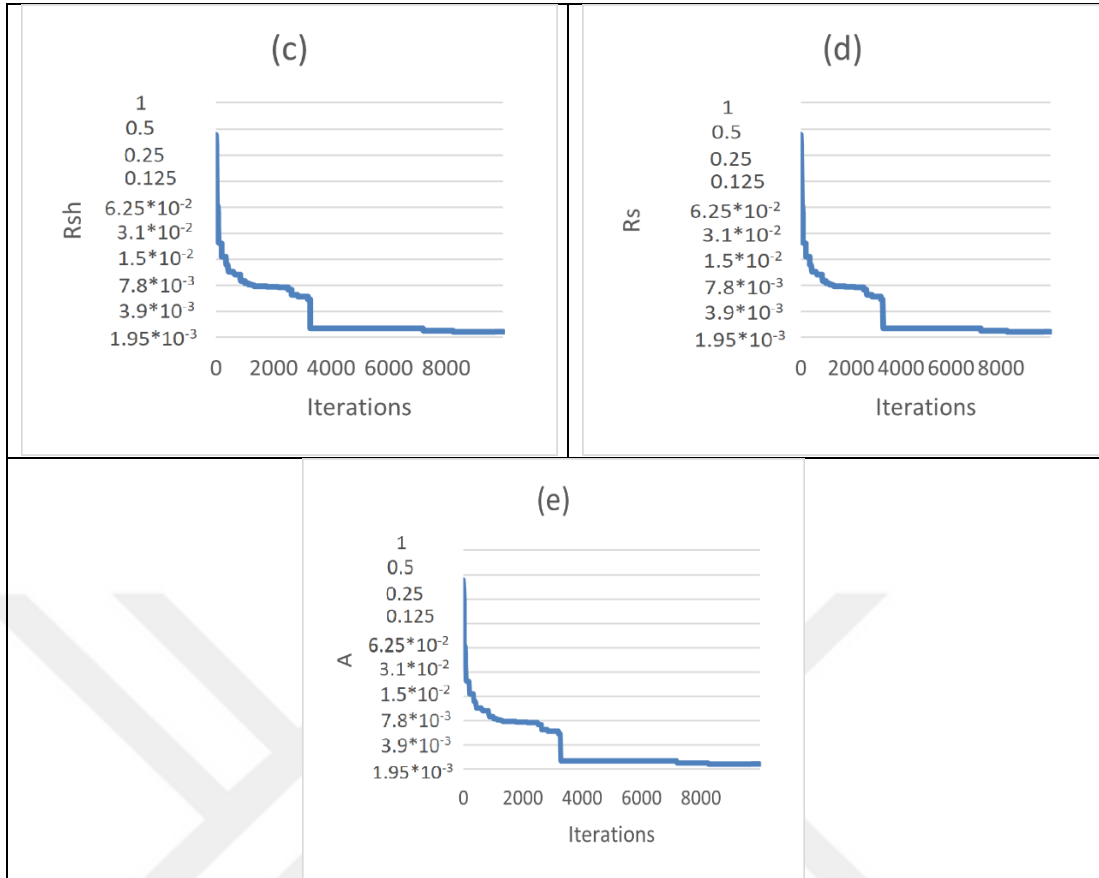


Figure 14: The line charts for the five values produced by CHIO representing the Power Watt PWP-201's properties.

For the Power Watt PWP-201 equivalent circuit elements, figure 10 (a-e), the algorithm's journeys didn't increase overall drastically. Instead, for all the parameters, CHIO has taken an exponential exploration drop followed by a vertical one downward, reaching a plateau right before the 4000th try; the algorithm did not want to change the value again till reaching near double the number of iterations, settling into the final output at about 80% of the allowed iterations limit of ten thousand, which is very notable since the algorithm almost did not need that large number of guesses for RTC France's two versions of models.

Table 5: Power Watt PWP-201 estimated parameters' RMSE by CHIO followed by the most recent successful algorithms' results RMSE accompanied by their setup specifications.

Method	Population Size	Iterations	Runs
CHIO	25	10000	30
FPA	25	1000	Unspecified
COA¹	100	10000	50
ICSO	15	5000	100
PSOCS	10,20,30,40,50,60	12000-14000	20000
TPTLBO	50	Unspecified	30
IGWO 2021	15	25000	50
WHHO	30	5000	30

¹ Coyote optimization algorithm

3.4. Statistical Analysis

In table 6, a statistical overview of the previously mentioned results can be found; the minimum, average, and maximum RMSE values of each CHIO group of runs show a considerable convergence rate, which proves the algorithm's flexibility.

Table 6: The best, worst, and average RMSE from all the runs of CHIO

RTC France			
RMSE	SDM	DDM	Power Watt PWP-201
Minimum	$7.75 \cdot 10^{-3}$	$7.48 \cdot 10^{-4}$	$2.27 \cdot 10^{-3}$
Maximum	$1.02 \cdot 10^{-3}$	$9.98 \cdot 10^{-4}$	$8.32 \cdot 10^{-3}$
Average	$8.36 \cdot 10^{-4}$	$7.97 \cdot 10^{-4}$	$4.66 \cdot 10^{-3}$

The table shows an impressive minimum and average value that puts CHIO among the top-performing algorithms, although having a reduced maximum value would have made CHIO climb to the top of the charts in terms of ruggedness but at the same time would lessen the algorithm’s flexibility and exploration abilities. Figures 11 and 12 illustrate CHIO’s best fitness function value for every one of the 30 runs.

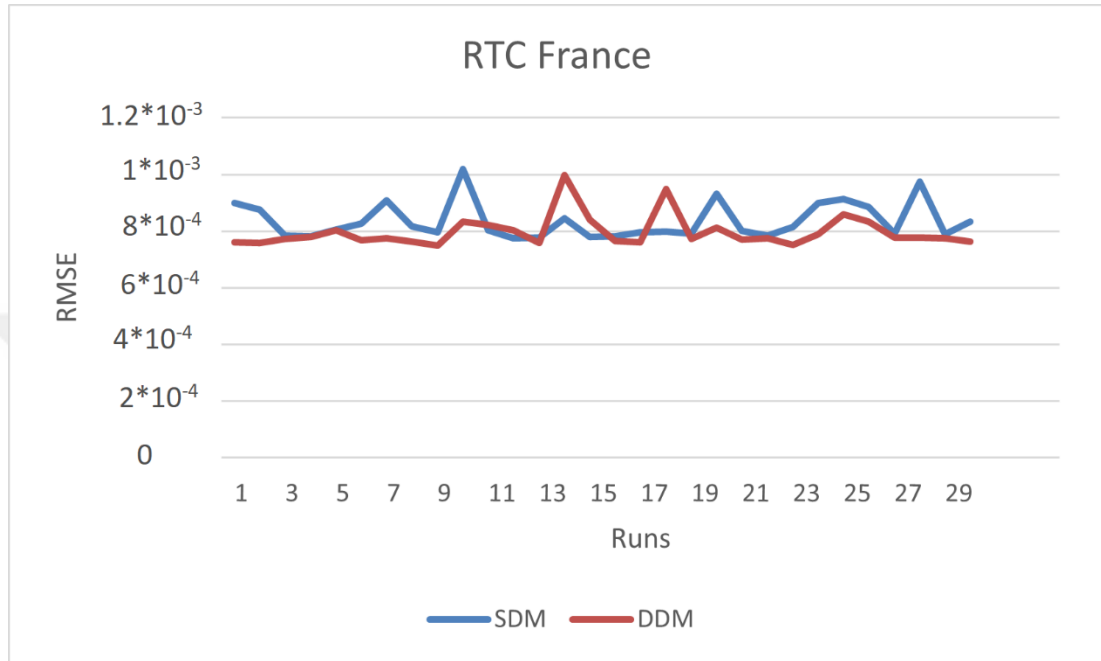


Figure 15: the average RMSE values exerted by CHIO over the total 30 runs made for the RTC France single and double diode models.

The figure above shows a high variability resemblance for both the SDM and DDM models, which confirms CHIO’s reliability when confronted by a higher number of parameters to predict.

On the other hand, the RMSE variability in figure 12 tells another story for the Power Watt PWP-201 model; the wider gaps between the RMSE values over 30 runs were worrisome; astonishingly, the very deep dips seen below have exerted results very comparable to state-of-the-art algorithms’ results.

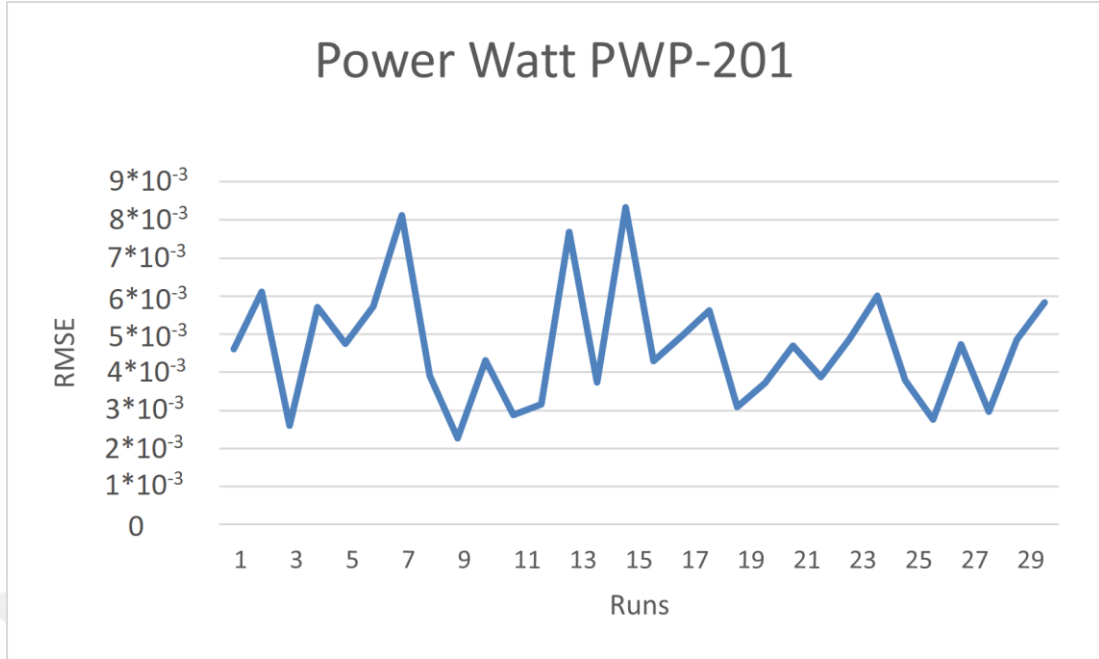


Figure 16: The fitness function for the parameters extracted by CHIO for the Power Watt PWP-201 model over the 30 runs.

3.5. Performance and Runtime

The following table demonstrates the total run time needed for achieving one complete run of CHIO estimating PV cell parameters, the algorithmic parameters set for each PV model were as specified in the results section with the exemption of the number of runs, and the timings below were taken from MATLAB by using the function “Run and Time”.

Table 7: The timings are taken from MATLAB for one complete run of CHIO estimating PV cell models’ parameters.

PV Cell Model	RTC France SDM	RTC France DDM	Power-Watt PWP201
Total Runtime	70.853s	95.633s	171.766s

The timings above show that CHIO has very efficient code that can achieve very impressive performance metrics, which would be timesaving and expands the horizon to optimize more complex functions without sacrificing the user time and with less energy consumption which is crucial.

3.6. Literature Algorithms

In this section, CHIO's performance will be compared against some of the state-of-the-art algorithms that have been studied in the literature in recent years, as presented in table 8. The main element of the comparison is the fitness function value, which is also known as the root mean square error (equation 20), of the following parameters extracted by each algorithm:

- (I_{ph} , I_{sd} , R_s , R_{sh} , & a) for the RTC France and the Power Watt PWP-201 single diode model equivalent circuits.
- (I_{ph} , I_{sd1} , I_{sd2} , R_s , R_{sh} , a_1 & a_2) for the RTC France double diode model variant.

This comparison is essential to this study as it presents an opportunity to benchmark CHIO's performance and the viability of its results.

Table 8: RMSE of results extracted by CHIO and algorithms used in recent literature.

Algorithm	RTC France SDM	RTC France DDM	Power-Watt PWP201
CHIO	$7.75 \cdot 10^{-4}$	$7.48 \cdot 10^{-4}$	$2.27 \cdot 10^{-3}$
FPA	$7.73 \cdot 10^{-4}$	$7.84 \cdot 10^{-4}$	$2.05 \cdot 10^{-3}$
COA¹	$9.86 \cdot 10^{-4}$	$9.82 \cdot 10^{-4}$	$4.66 \cdot 10^{-3}$
COA²	$7.73 \cdot 10^{-4}$	$7.33 \cdot 10^{-4}$	$2.05 \cdot 10^{-3}$

ICSO	9.86*10 ⁻⁴	9.83*10 ⁻⁴	2.43*10 ⁻³
EHHO	6.43*10 ⁻⁴	9.74*10 ⁻⁴	7.21*10 ⁻⁴
PSOCS	9.86*10 ⁻⁴	9.83*10 ⁻⁴	2.43*10 ⁻³
TPTLBO	9.86*10 ⁻⁴	9.82*10 ⁻⁴	2.43*10 ⁻³
IGWO	9.86*10 ⁻⁴	9.82*10 ⁻⁴	2.43*10 ⁻³
WHHO	9.86*10 ⁻⁴	9.82*10 ⁻⁴	2.42*10 ⁻³

¹ Chaotic Optimization Approach

² Coyote optimization algorithm

First, The Flower Pollination Algorithm (FPA) by (Alam vd., 2015) FPA has achieved a remarkable RMSE for the RTC France Single Diode Model and the Power Watt PWP-201, which is slightly more optimal than CHIO's result for the same diode model; as for the RTC France Double Diode Model, CHIO has achieved an excellent RMSE that even surpassed the very remarkable results predicted by FPA.

Next on the list is the Chaotic Optimization Approach (COA) by (Calasan vd., 2019) which has achieved outstanding results for the RTC France (Single & Double Diode Models), but these results were not as close to the desired outcome and have been lapped by CHIO's RMSE regarding the two models mentioned above.

At number three, The Coyote Optimization Algorithm (COA) (Chin & Salam, 2019) sits with results nearly identical to the first algorithm (FPA), with the exemption of the Double Diode Model of the RTC France solar cell surpassing CHIO's RMSE in all three models by a very slight margin.

The fourth algorithm to compare is the Improved Cuckoo Search Optimization (ICSO) (Gude & Jana, 2020) which has produced results with RMSE like the second-mentioned algorithm and has been passed by CHIO's RMSE in all three PV Cell models.

As for diversification-enriched Harris hawks' optimization with chaotic drifts (I-HHO) by (Chen vd., 2020) had great success with the Single Diode Model of the RTC France surpasses CHIO's RMSE a bit but lagged with regards to the Double Diode Model of the same manufacturer.

Random reselection particle swarm optimization (PSOCS) by (Fan vd., 2022) produced very consistent results for the single and double diode models of the RTC France but did not surpass CHIO's results' RMSE in all three models.

Number Seven is the Triple-Phase Teaching-Learning-Based

Optimization (TPTLBO) by (Liao vd., 2020) has given results with RMSE at the same level as numerous algorithms, and it was very homogenous to each other; CHIO has provided a better RMSE for all the tested diode models.

IGWO is one of the most recent algorithms to be tested to extract PV Cell parameters; it stands for Grey Wolf Optimizer with Dimension Learning-Based Hunting Search Strategy by (Yesilbudak, 2021), and it provides parameters comparable to multiple other successful algorithms, and CHIO has slightly passed its results' RMSE.

Finally comes the Whippy Harris Hawks Optimization Algorithm (WHHO) by (Naeijian, Rahimnejad, Ebrahimi, Pourmousa ve Gadsden, 2021); it was also one of the new literature pieces to discuss the viability of an algorithm to extract PV Cell parameters and has resulted in a very equivalent RMSE to other algorithms and have also been outdone by CHIO's RMSE but not by much.

3.7. Statistical Analysis

Table 9 analyzes the results' RMSE for the generated PV Cell parameters by CHIO and other algorithms tested by the literature.

Table 9: The aggregated RMSE of all CHIO runs followed by the sample of algorithms to benchmark the performance.

Algorithm	RMSE	RTC France SDM	RTC France DDM	Power-Watt PWP201
CHIO	Min.	$7.75 \cdot 10^{-4}$	$7.48 \cdot 10^{-4}$	$2.27 \cdot 10^{-3}$
	Max.	$1.02 \cdot 10^{-3}$	$9.98 \cdot 10^{-4}$	$8.32 \cdot 10^{-3}$
	Avg.	$8.36 \cdot 10^{-4}$	$7.97 \cdot 10^{-4}$	$4.66 \cdot 10^{-3}$
ICSO	Min.	$9.86 \cdot 10^{-4}$	$9.83 \cdot 10^{-4}$	$2.43 \cdot 10^{-3}$
	Max.	$9.86 \cdot 10^{-4}$	$1.10 \cdot 10^{-3}$	$2.43 \cdot 10^{-3}$
	Avg.	$9.86 \cdot 10^{-4}$	$9.95 \cdot 10^{-4}$	$2.43 \cdot 10^{-3}$
PSOCS	Min.	$9.86 \cdot 10^{-4}$	$9.83 \cdot 10^{-4}$	$2.43 \cdot 10^{-3}$
	Max.	$9.86 \cdot 10^{-4}$	$1.41 \cdot 10^{-3}$	$2.43 \cdot 10^{-3}$
	Avg.	$9.86 \cdot 10^{-4}$	$1.03 \cdot 10^{-3}$	$2.43 \cdot 10^{-3}$
TPTLBO	Min.	$9.86 \cdot 10^{-4}$	$9.82 \cdot 10^{-4}$	$2.43 \cdot 10^{-3}$
	Max.	$9.86 \cdot 10^{-4}$	$9.86 \cdot 10^{-4}$	$2.43 \cdot 10^{-3}$
	Avg.	$9.86 \cdot 10^{-4}$	$9.84 \cdot 10^{-4}$	$2.43 \cdot 10^{-3}$
EHHO	Min.	$6.43 \cdot 10^{-4}$	$9.74 \cdot 10^{-4}$	$7.21 \cdot 10^{-4}$
	Max.	$7.60 \cdot 10^{-4}$	$9.78 \cdot 10^{-4}$	$7.87 \cdot 10^{-4}$
	Avg.	$7.32 \cdot 10^{-4}$	$9.44 \cdot 10^{-4}$	$6.43 \cdot 10^{-4}$
WHHO	Min.	$9.8602 \cdot 10^{-4}$	$9.8248 \cdot 10^{-4}$	$2.4250 \cdot 10^{-3}$
	Max.	$9.8602 \cdot 10^{-4}$	$9.8250 \cdot 10^{-4}$	$2.4250 \cdot 10^{-3}$

Avg.	$9.8602 \cdot 10^{-4}$	$9.8249 \cdot 10^{-4}$	$2.4250 \cdot 10^{-3}$
------	------------------------	------------------------	------------------------

For the total of 30 Runs, CHIO's best result for each run did not deviate much, apart from the 10th run for the single diode model of the RTC France solar cell, where it had an anomaly RMSE of $1.02 \cdot 10^{-3}$, it could have been an exploration run or could be a motive for future modification for the algorithm.

As for the other algorithms, some of the papers used in the prior comparison did not include their largest and average RMSE; therefore, they will not be incorporated.

It was observed that most of the algorithms in the table had very high robustness, although, for the most part, their best results did not exceed CHIO's best RMSE results, which shows CHIO's high flexibility and exceptional exploration ability.

CONCLUSION AND RECOMMENDATIONS

The adverse effects of using fossil fuels have been discussed in this work, followed by alternative energy sources as solutions. Next, the drawbacks of solar energy alongside the possible solutions, specifically PV module modeling and parameter extractions using optimization algorithms.

The CHIO algorithm and its many stages of operation were presented in the second chapter. The algorithm was then rigorously tested by being run with various combinations of algorithmic parameters; the best combination was then selected to demonstrate the algorithm's capacity to predict and extrapolate the unknown parameters of PV Cells, which are the constituents of the equivalent circuit representing the PV cells.

In order to ensure the output was the most optimal, the fitness function, or RMSE, of the extracted results was obtained by running the algorithm with various settings for each set of runs. The RMSE was then compared to the RMSE of the results extracted by the state-of-the-art algorithms worked on recently in the literature.

CHIO has demonstrated adaptability and an excellent balance between exploitation and exploration skills, producing outcomes that are quite competitive with the best metaheuristic optimization performance.

Future research should test CHIO to simulate PV Cells with a wider variety of PV Cell efficiencies and different shading situations.

It is strongly advised to investigate CHIO's capability to predict its parameters using physical PV cells.

Also, the algorithm could be modified or hybridized with another optimization algorithm that is also population-based; it could result in an even more impressive and groundbreaking outcome.

It is well known that incorporating a TRIZ-inspired operator into any population-based algorithm could lead to even better results(Al-Betar vd., 2020); therefore, it is recommended that CHIO should be tested with an incorporated TRIZ-inspired operator.

REFERENCES

- Alam, D. F., Yousri, D. A., & Eteiba, M. B. (2015). Flower Pollination Algorithm based solar PV parameter estimation. *Energy Conversion and Management*, *101*. <https://doi.org/10.1016/j.enconman.2015.05.074>
- Al-Betar, M. A., Alomari, O. A., & Abu-Romman, S. M. (2020). A TRIZ-inspired bat algorithm for gene selection in cancer classification. *Genomics*, *112*(1). <https://doi.org/10.1016/j.ygeno.2019.09.015>
- Al-Betar, M. A., Alyasseri, Z. A. A., Awadallah, M. A., & Abu Doush, I. (2021). Coronavirus herd immunity optimizer (CHIO). *Neural Computing and Applications*, *33*(10). <https://doi.org/10.1007/s00521-020-05296-6>
- Allam, D., Yousri, D. A., & Eteiba, M. B. (2016). Parameters extraction of the three diode model for the multi-crystalline solar cell/module using Moth-Flame Optimization Algorithm. *Energy Conversion and Management*, *123*. <https://doi.org/10.1016/j.enconman.2016.06.052>
- Bhattacharyya, T., Chatterjee, B., Singh, P. K., Yoon, J. H., Geem, Z. W., & Sarkar, R. (2020). Mayfly in Harmony: A new hybrid meta-heuristic feature selection algorithm. *IEEE Access*, *8*. <https://doi.org/10.1109/ACCESS.2020.3031718>
- Ćalasan, M., Jovanović, D., Rubežić, V., Mujović, S., & Dukanović, S. (2019). Estimation of single-diode and two-diode solar cell parameters by using a chaotic optimization approach. *Energies*, *12*(21). <https://doi.org/10.3390/en12214209>
- Callier, P., & Sandel, O. (2021). Introduction to Artificial Intelligence. *Actualites Pharmaceutiques*, *60*(611). <https://doi.org/10.1016/j.actpha.2021.10.005>
- Chen, H., Jiao, S., Wang, M., Heidari, A. A., & Zhao, X. (2020). Parameters identification of photovoltaic cells and modules using diversification-enriched Harris hawks optimization with chaotic drifts. *Journal of Cleaner Production*, *244*. <https://doi.org/10.1016/j.jclepro.2019.118778>
- Chin, V. J., & Salam, Z. (2019). Coyote optimization algorithm for the parameter extraction of photovoltaic cells. *Solar Energy*, *194*. <https://doi.org/10.1016/j.solener.2019.10.093>
- Easwarakhanthan, T., Bottin, J., Bouhouch, I., & Boutrif, C. (1986). Nonlinear Minimization Algorithm for Determining the Solar Cell Parameters with Microcomputers. *International Journal of Solar Energy*, *4*(1). <https://doi.org/10.1080/01425918608909835>
- Fan, Y., Wang, P., Heidari, A. A., Chen, H., HamzaTurabieh, & Mafarja, M. (2022). Random reselection particle swarm optimization for optimal design of solar photovoltaic modules. *Energy*, *239*. <https://doi.org/10.1016/j.energy.2021.121865>

- Green, M. A., Dunlop, E. D., Hohl-Ebinger, J., Yoshita, M., Kopidakis, N., & Hao, X. (2022). Solar cell efficiency tables (version 59). *Progress in Photovoltaics: Research and Applications*, 30(1). <https://doi.org/10.1002/pip.3506>
- Gude, S., & Jana, K. C. (2020). Parameter extraction of photovoltaic cell using an improved cuckoo search optimization. *Solar Energy*, 204. <https://doi.org/10.1016/j.solener.2020.04.036>
- Humada, A. M., Hojabri, M., Mekhilef, S., & Hamada, H. M. (2016). Solar cell parameters extraction based on single and double-diode models: A review. *Çinde Renewable and Sustainable Energy Reviews* (C. 56). <https://doi.org/10.1016/j.rser.2015.11.051>
- Ishaque, K., & Salam, Z. (2011). An improved modeling method to determine the model parameters of photovoltaic (PV) modules using differential evolution (DE). *Solar Energy*, 85(9). <https://doi.org/10.1016/j.solener.2011.06.025>
- Ishaque, K., Salam, Z., & Taheri, H. (2011). Simple, fast and accurate two-diode model for photovoltaic modules. *Solar Energy Materials and Solar Cells*, 95(2). <https://doi.org/10.1016/j.solmat.2010.09.023>
- Jenkins, A., Gupta, V., Myrick, A., & Lenoir, M. (2019). *Variations of Genetic Algorithms*.
- Jervase, J. A., Bourdoucen, H., & Al-Lawati, A. (2001). Solar cell parameter extraction using genetic algorithms. *Measurement Science and Technology*, 12(11). <https://doi.org/10.1088/0957-0233/12/11/322>
- Jiang, L. L., Maskell, D. L., & Patra, J. C. (2013). Parameter estimation of solar cells and modules using an improved adaptive differential evolution algorithm. *Applied Energy*, 112. <https://doi.org/10.1016/j.apenergy.2013.06.004>
- Katoch, S., Chauhan, S. S., & Kumar, V. (2021). A review on genetic algorithm: past, present, and future. *Multimedia Tools and Applications*, 80(5), 8091-8126. <https://doi.org/10.1007/s11042-020-10139-6>
- Khanna, V., Das, B. K., Bisht, D., Vandana, & Singh, P. K. (2015). A three diode model for industrial solar cells and estimation of solar cell parameters using PSO algorithm. *Renewable Energy*, 78. <https://doi.org/10.1016/j.renene.2014.12.072>
- Korpela, S. A. (2006). Oil depletion in the world. *Çinde Current Science* (C. 91, Issue 9).
- Liao, Z., Chen, Z., & Li, S. (2020). Parameters Extraction of Photovoltaic Models Using Triple-Phase Teaching-Learning-Based Optimization. *IEEE Access*, 8. <https://doi.org/10.1109/ACCESS.2020.2984728>

- Mi, Z., Chen, J., Chen, N., Bai, Y., Fu, R., & Liu, H. (2016). Open-loop solar tracking strategy for high concentrating photovoltaic systems using variable tracking frequency. *Energy Conversion and Management*, 117. <https://doi.org/10.1016/j.enconman.2016.03.009>
- Moshksar, E., & Ghanbari, T. (2017). Adaptive Estimation Approach for Parameter Identification of Photovoltaic Modules. *IEEE Journal of Photovoltaics*, 7(2). <https://doi.org/10.1109/JPHOTOV.2016.2633815>
- Naeijian, M., Rahimnejad, A., Ebrahimi, S. M., Pourmousa, N., & Gadsden, S. A. (2021). Parameter estimation of PV solar cells and modules using Whippy Harris Hawks Optimization Algorithm. *Energy Reports*, 7. <https://doi.org/10.1016/j.egyr.2021.06.085>
- Sivanandam, S. N., & Deepa, S. N. (2008). Chapter 2 Genetic Algorithms. *Introduction to Genetic Algorithms*.
- Yesilbudak, M. (2021). Parameter extraction of photovoltaic cells and modules using grey wolf optimizer with dimension learning-based hunting search strategy. *Energies*, 14(18). <https://doi.org/10.3390/en14185735>
- Zekry, A., Shaker, A., & Salem, M. (2018). Solar Cells and Arrays: Principles, Analysis, and Design. İçinde *Advances in Renewable Energies and Power Technologies* (C. 1). <https://doi.org/10.1016/B978-0-12-812959-3.00001-0>

